Supporting Information[i]

Triptycene as a Supramolecular Additive in PTB7:PCBM blends and its Influence on Photovoltaic Properties

Lethy Krishnan Jagadamma[1], Liam J. McCarron[2], Alan A. Wiles[2], Victoria Savikhin[3, 4], Muhammad T. Sajjad[1], Mahdieh Yazdani[5], Vincent M. Rotello[5], Michael F. Toney[3], Graeme Cooke*[2], Ifor D. W. Samuel*[1]

[1]Organic Semiconductor Centre, SUPA, School of Physics and Astronomy, University of St. Andrews, St. Andrews, Fife, KY16 9SS (UK)

[2]Glasgow Centre for Physical Organic Chemistry (GCPOC), WestCHEM, School of Chemistry, University of Glasgow, Glasgow, G12 8QQ, UK.

[3] Stanford Synchrotron Radiation Lightsource, SLAC National Accelerator Laboratory, 2575 Sand Hill Road, Menlo Park, CA 94025, United States

[4]Electrical Engineering Department, Stanford University, 350 Serra Mall, Stanford, CA 94305

[5]Department of Chemistry, University of Massachusetts Amherst, 710 North Pleasant Street, Amherst, Massachusetts 01003, United States

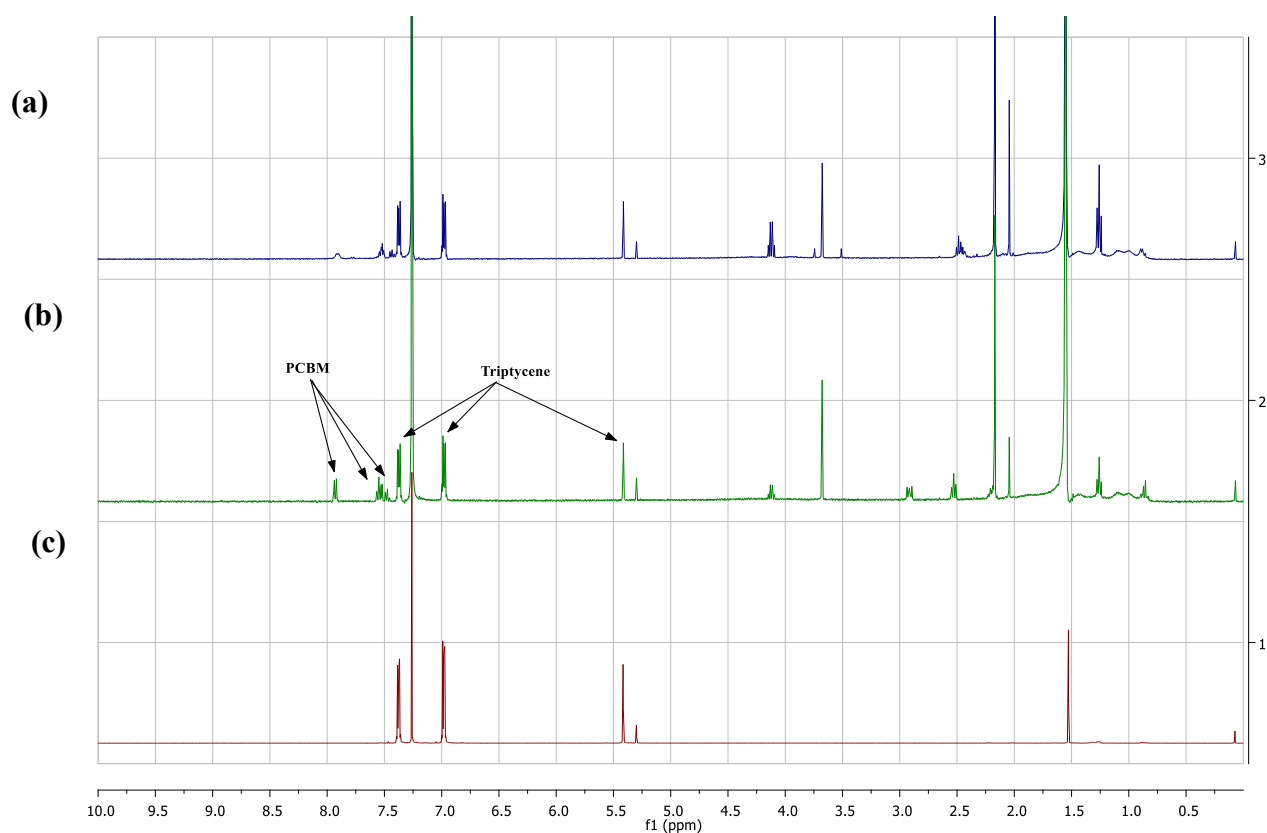*E-mail: idws@st-andrews.ac.uk; Graeme.Cooke@glasgow.ac.uk

Figure S1 ^{1}H NMR spectra of PTB7-Fullerene-TPC blends (400 MHz, CDCl$_3$, 25 ^{o}C, TMS): a) PTB7-PC$_{71}$BM-TPC blend. b) PTB7-PC$_{61}$BM-TPC blend and c) Neat triptycene. Triptycene and aromatic PCBM peaks have been highlighted for clarity.

The presence of Triptycene in the BHJ films after completion of the device fabrication is confirmed by ^{1}H NMR (Figure S1). Here, the presence of triptycene is clearly evident and confirms that TPC remains in both PTB7:PC$_{61}$BM:TPC and PTB7:PC$_{71}$BM:TPC blends even after the completion of the solar cell device fabrication.

Table S1. Photovoltaic properties (average of 6-10 devices) of the PTB7:PC$_{61}$BM blends as a function of different loadings of TPC content.

| TPC (conc.) (mg/mL)	J_{sc} (mA/cm^2)	V_{oc} (V)	FF (%)	R_{sh} (Ωcm^2)	R_s (Ωcm^2)	PCE Avg. (%)	PCE Best (%)
0	11.3±0.5	0.753±0.009	38.6±1.1	193±30	3.40±1.1	3.28±0.30	3.53
0.05	11.5±0.3	0.753±0.004	40.6±1.2	256±31	3.26±0.8	3.33±0.23	3.64
0.25	11.4±0.6	0.753±0.003	43.2±0.8	302±32	2.98±1.3	3.47±0.19	3.73
0.5	11.8±0.3	0.762±0.005	43.9±0.9	322±26	3.5±0.5	3.60±0.32	4.03
2.5	12.1±0.3	0.776±0.010	52.5±1.1	479±107	3.82±0.4	4.90±0.25	5.20
5	12.1±0.3	0.777±0.010	54.8±0.6	527±51	3.51±0.2	5.14±0.28	5.50
7.5	12.0±0.3	0.791±0.010	57.8±0.4	692±52	1.69±0.3	5.42±0.27	5.70
12.5	11.6±0.7	0.795±0.010	53.6±1.6	578±143	1.87±0.26	4.93±0.16	5.10
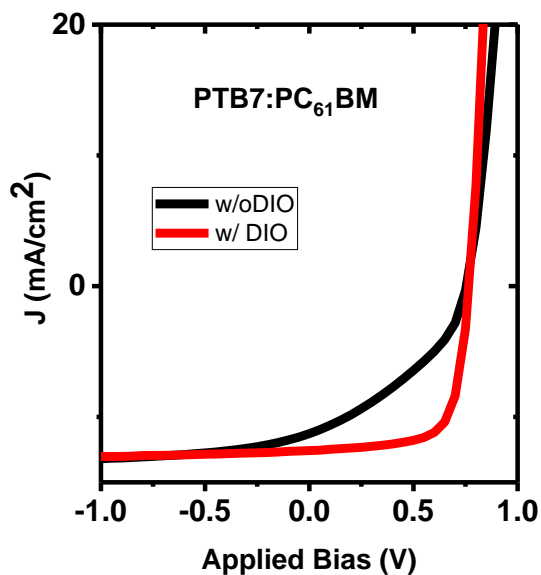
Figure S2 J-V characteristics of the PTB7:PC$_{61}$BM blends with 3% DIO and without DIO

Table S2. Photovoltaic properties (averaged over 6 devices) of the PTB7:PC$_{61}$BM blends with and without DIO additive.

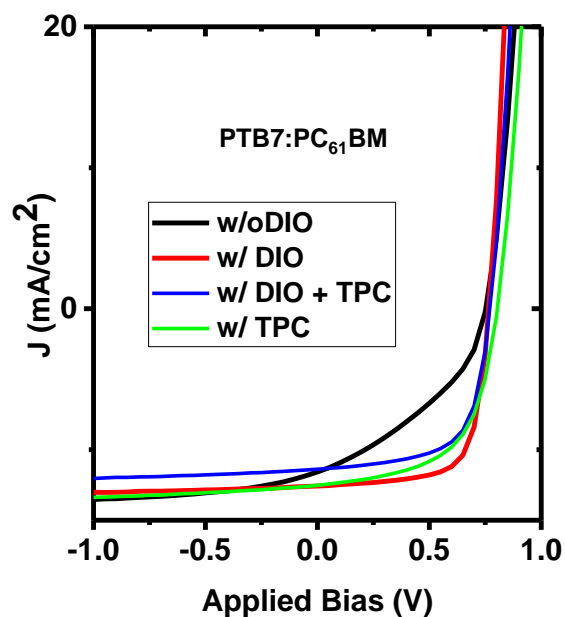| PTB7: PC$_{61}$BM	J_{sc} (mA/cm^2)	V_{oc} (V)	FF (%)	R_{sh} (Ωcm^2)	R_s (Ωcm^2)	PCE (%) avg.	PCE max (%)
No DIO	11.4±1.0	0.753±0.009	38.6±1.1	193±30	3.40±1.1	3.28±0.30	3.53
3 % DIO	12.2±0.7	0.755±0.008	70.0±0.9	1230±313	1.6±0.2	6.44±0.40	6.81

Figure S3. J-V characteristics showing the combined effect of TPC and DIO additive

Table S3. Photovoltaic properties (averaged over 6-8 devices) of the PTB7:$PC_{61}BM$ blends as a function of combined effect of TPC and DIO.

PTB7: $PC_{61}BM$	J_{sc} (mA/cm^2)	V_{oc} (V)	FF (%)	PCE (%) avg.	PCE max (%)
No DIO	11.2	0.753	38.6	3.22	3.53
TPC	12.0	0.791	58.5	5.42	5.70
3 % DIO	12.2	0.755	70.0	6.44	6.81
3%DIO+TPC	11.8	0.772	64.9	5.56	5.87

Table S4. Photovoltaic properties (averaged over 6-10 devices) of the PTB7:PC$_{71}$BM blends as a function of different loadings of TPC incorporation.

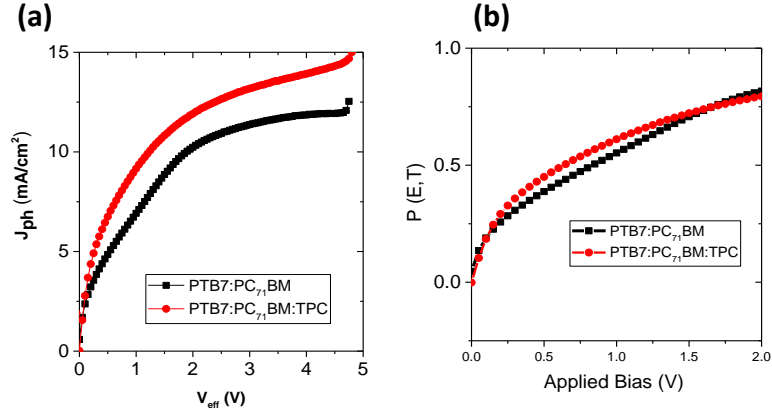| TPC (conc.) (mg/mL)	J_{sc} (mA/cm^2)	V_{oc} (V)	FF (%)	PCE avg. (%)	PCE (%)
0	8.16±0.38	0.76±00.01	35.6±0.92	2.22±0.09	2.33
2.5	8.76±0.39	0.75±0.01	34.3±0.41	2.27±0.16	2.42
5	8.45±0.29	0.77±0.01	36.2±0.69	2.34±0.08	2.44
7.5	9.45±0.43	0.76±0.01	38.6±1.6	2.78±0.23	3.23
12.5	10.9±0.55	0.795±0.01	41.5±1.5	3.58±0.15	3.76
25	5.91±0.71	0.827±0.008	31.3±0.8	1.53±0.17	1.67

Figure S4: Comparison of the (a) photocurrent density (J_{ph}) and (b) dissociation probability $P(E,T)$ for PTB7:PC$_{71}$BM and PTB7:PC$_{71}$BM:TPC solar cells.

$$J_{ph} = J_L - J_D$$

J_{ph} is the photocurrent density and J_L and J_D are the current densities under illumination and dark respectively.
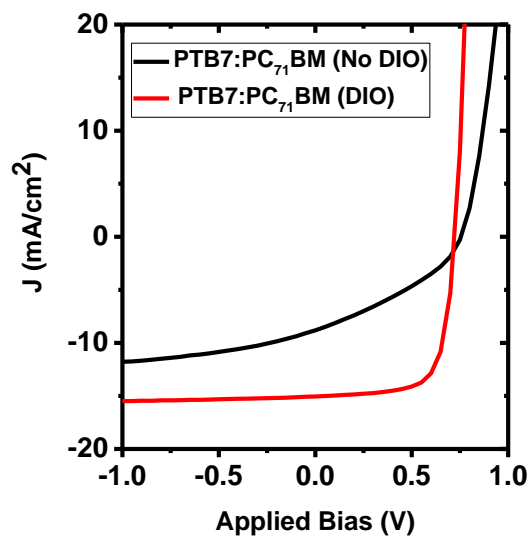
Figure S5. J-V characteristics of the PTB7:PC$_{71}$BM blends with 3% DIO and without DIO

Table S5. Photovoltaic properties (best devices) of the PTB7:PC$_{71}$BM blends with and without DIO additive.

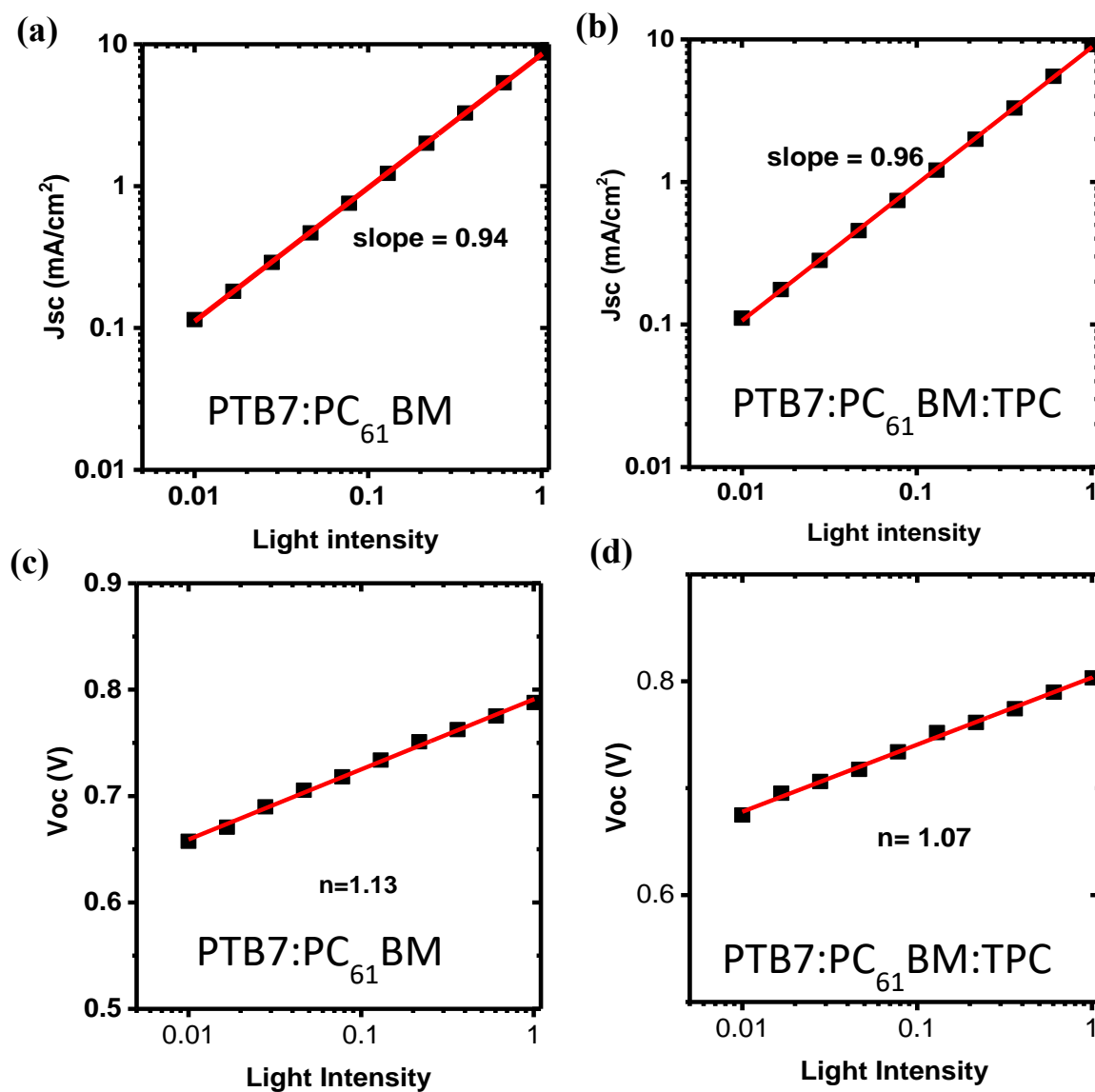| PTB7:PC$_{71}$BM	J_{sc} (mA/cm^2)	V_{oc} (V)	FF (%)	PCE(%)
No DIO	8.81	0.755	35	2.33
3 % DIO	15.3	0.715	71.3	7.81

Figure S6. (a) Short circuit current density, J_{sc} *vs* light intensity (on logarithmic scale) for PTB7:PC$_{61}$BM solar cells (b) Short circuit current density, J_{sc} *vs* light intensity (on logarithmic scale) for PTB7:PC$_{61}$BM solar cells with added TPC (c) open circuit voltage, V_{oc} *vs* light intensity (on semi-logarithmic scale) for PTB7:PC$_{61}$BM solar cells (c) open circuit voltage, V_{oc} *vs* light intensity (on semi-logarithmic scale) for PTB7:PC$_{61}$BM solar cells with added TPC.

The short circuit current density J_{sc} depends upon the light intensity I by a power law relation of

$$J_{SC} \propto I^{\alpha}$$

where α is a recombination factor and is unity when all the separated charges are collected to the electrodes. A small decrease of α from unity corresponds to weak bi-molecular recombination losses.[1-2] The values of α in the range of 0.7-0.8, however, corresponds to space charge effects. The variation of J_{sc} as a function of light intensity (log-log scale) is shown in **Figure S6**. For both neat and TPC added devices (under optimum conditions) J_{sc} dependence on light intensity shows a weak bimolecular recombination, with α values being 0.941±0.003 and 0.959±0.005 respectively. This implies that most of the charges generated at the short circuit conditions are swept out of the active layer to constitute current in the external circuit in both cases, though a slight weaker bimolecular recombination loss is observed for TPC containing PTB7:PC$_{61}$BM devices. So, measurements of the dependence of Jsc on light intensity suggest that bimolecular recombination plays a minor role to account for the improved performance of TPC containing devices. To gain further information about recombination mechanisms, the variation of Voc as a function of light intensity was studied. Voc is related to the incident light intensity through the relation: $V_{oc} = n \frac{k_B T}{q} \cdot ln(I)$ + constant, where k_B is the Boltzmann constant, n is the ideality factor, q is the charge and T is the temperature. When the slope of Voc versus the logarithm of the light intensity is $\frac{k_B T}{q}$ (n~1), the recombination mechanism that dominates is bimolecular recombination. A stronger dependence of Voc on light intensity corresponding to (n>1) indicates the presence of Shockley-Read-Hall (SRH) or trap assisted recombination competing with

bimolecular recombination.[2] In Figure S6(b), the plot of Voc *vs* light intensity (semi-logarithmic scale) is shown for both the PTB7:PC$_{61}$BM and the TPC:PTB7:PC$_{61}$BM devices. The slope obtained from these plots are respectively 1.13±0.01 and 1.07±0.01, and supporting that at open circuit conditions, bimolecular recombination dominates for both blends.
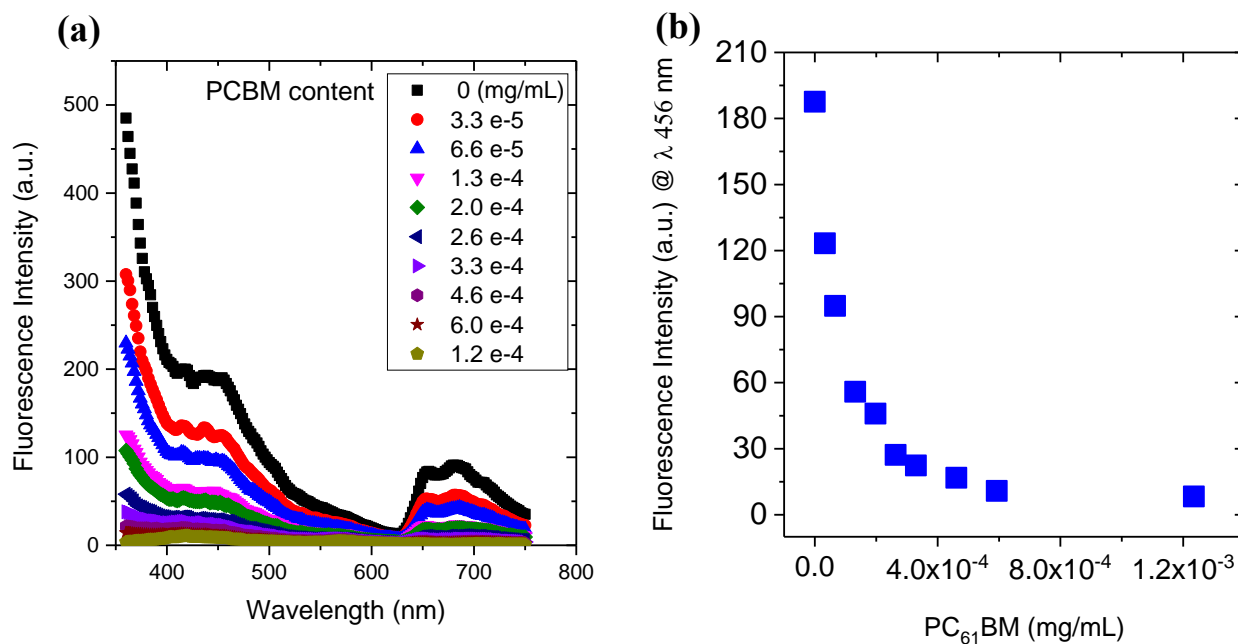

Figure S7. (a) Emission spectra of TPC in chlorobenzene solution and the effect of PC$_{61}$BM incorporation on the fluorescence spectra of TPC (b) the fluorescence quenching of TPC emission at 456 nm due to incorporation of PC$_{61}$BM in different concentration. The excitation wavelength used was 310 nm.
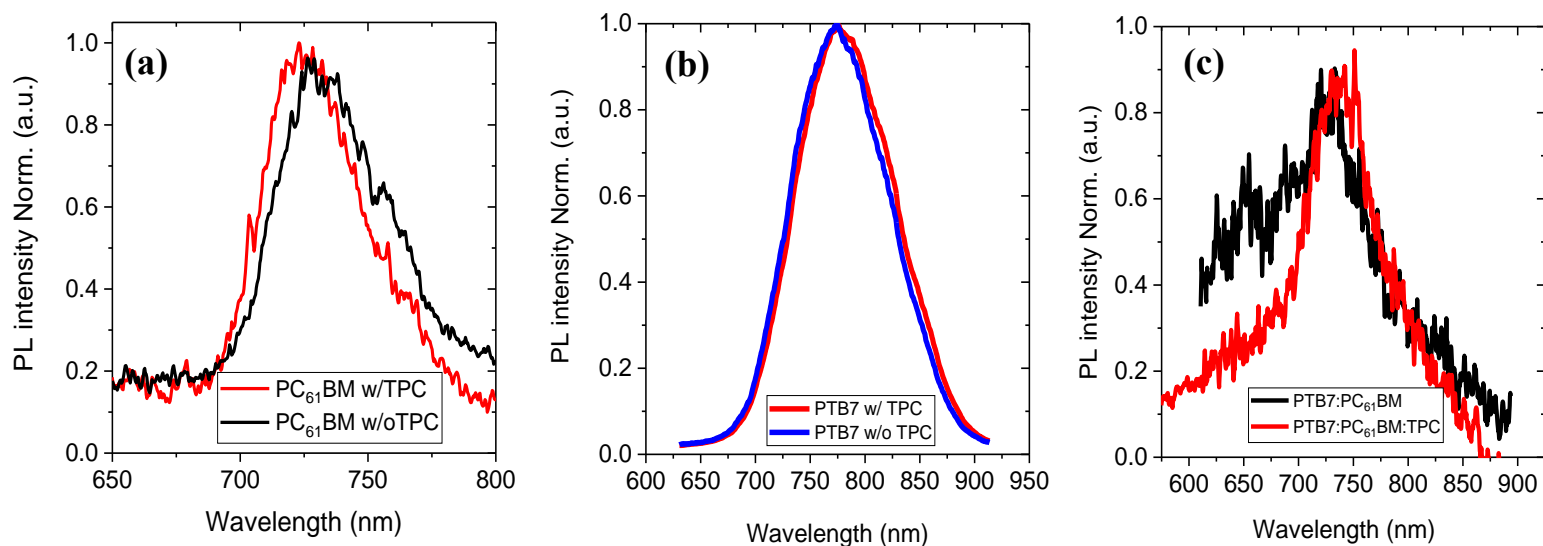
Figure S8: Steady state PL emission spectra of (a) $PC_{61}BM$ and TPC added $PC_{61}BM$ thin films (b) PTB7 and TPC:PTB7 thin films (c) PTB7:$PC_{61}BM$ and TPC incorporated PTB7:$PC_{61}BM$ blend films. The excitation wavelength is 515 or 650 nm.

The PL emission from the blend films shown in Figure S8(c) is mainly dominated by emission from fullerene molecules. However very noisy spectral feature of the PTB7:$PC_{61}BM$ blend films made it difficult to draw any conclusion on spectral shift due to TPC incorporation.
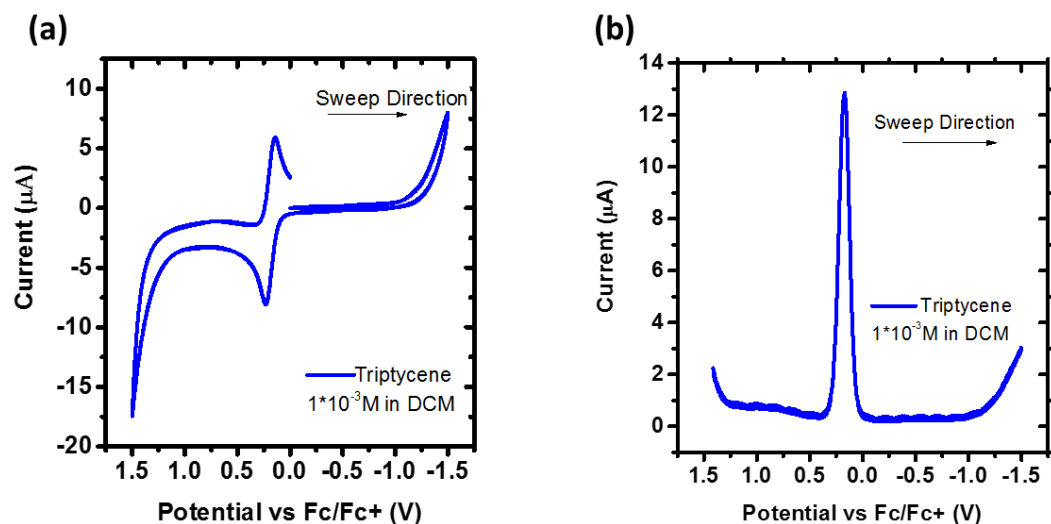
(a)

(b)

Figure S9: (a) Cyclic and (b) square wave voltammetry curves for TPC molecules (1 x 10^{-3} M in DCM). Ferrocene was used as an internal reference.
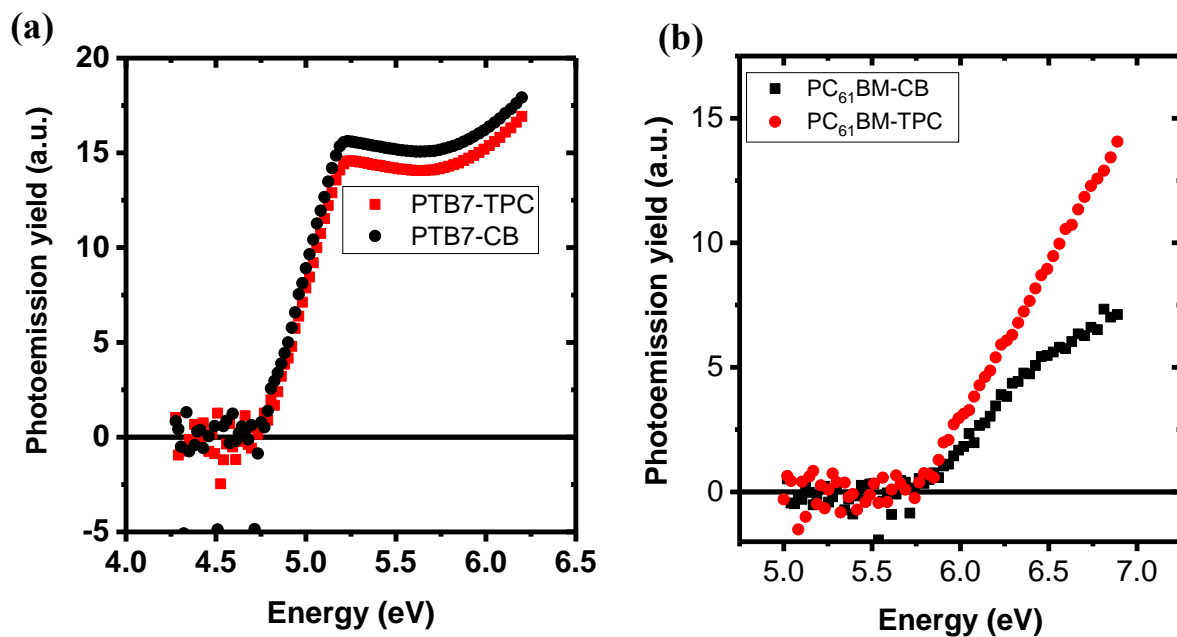
(a)

(b)

Figure S10: Air photoemission spectra of neat and TPC added (a) PTB7 and (b) PC$_{61}$BM thin films

The lower energy of the HOMO level of the PTB7 (-4.75 eV) thin films measured by APS compared to the previously reported HOMO levels of PTB7 (-5.2 eV), (mainly by CV measurements on PTB7 solutions) could be due to differences in measurement technique and methodology applied.[3-4] No difference in onset of photoemission yield is observed due to TPC incorporation in $PC_{61}BM$ as well as in PTB7.
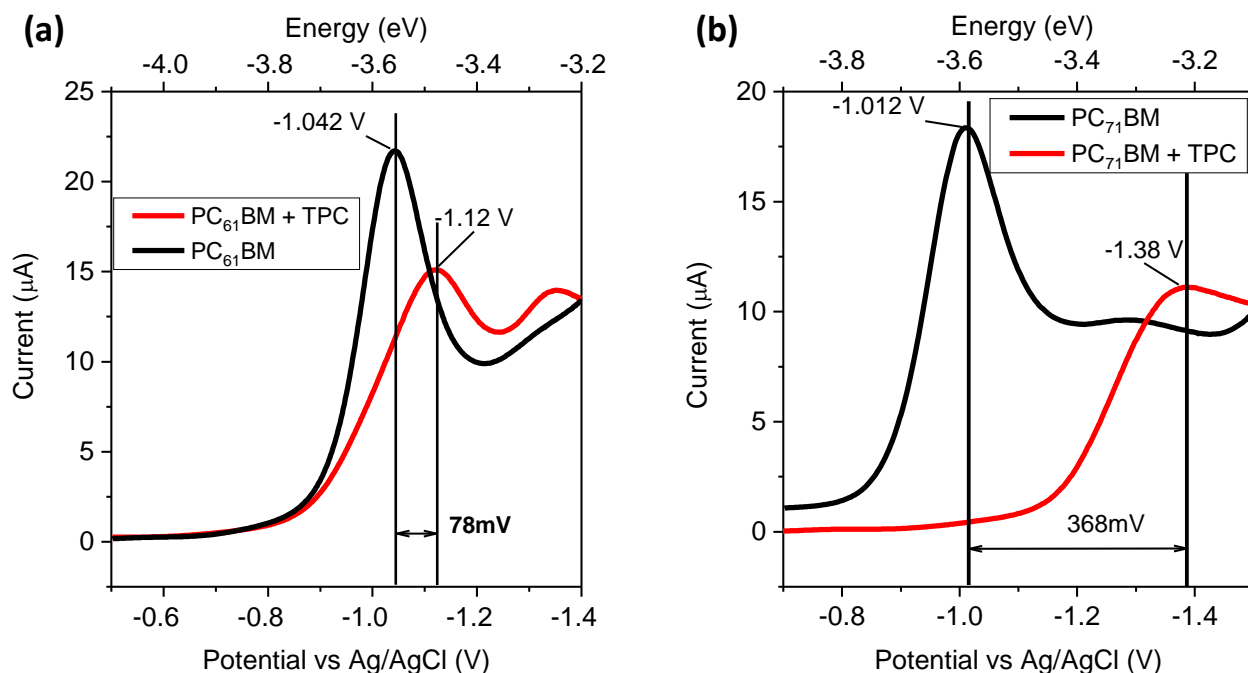

Figure S11: (a) Squarewave voltammogram of $PC_{61}BM$ films with and without TPC added (b) Squarewave voltammogram of $PC_{71}BM$ films with and without TPC added.
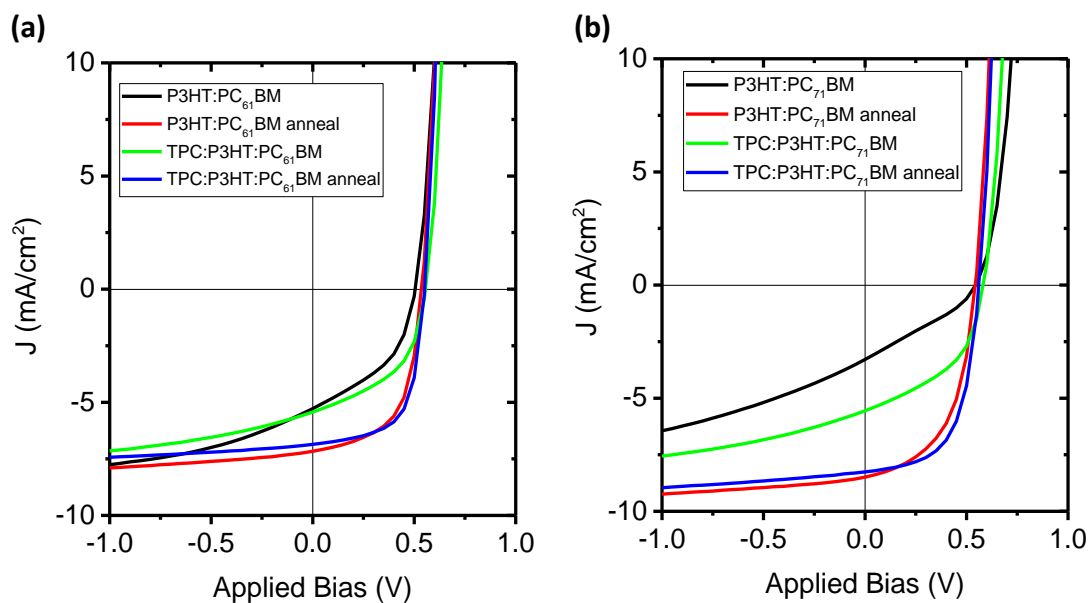
Figure S12: J-V characteristics of the (a) P3HT:PC$_{61}$BM and (b) P3HT:PC$_{71}$BM solar cells with and without TPC incorporation. The J-V curves corresponding to the effect of TPC in thermally annealed blend are also included.

Table S6: Photovoltaic performance parameters (average of 16 devices) of P3HT:PC$_{61}$BM devices with and without TPC incorporation

P3HT: PC$_{61}$BM	J$_{sc}$ (mA/cm^2)	V$_{oc}$ (V)	FF (%)	R$_{sh}$ (Ωcm^2)	R$_s$ (Ωcm^2)	PCE Avg.(%)	PCE max (%)
No anneal	5.19±0.14	0.486±0.018	43.47±0.45	223±15	1.27±0.23	1.10±0.06	1.19
Anneal	6.92±0.18	0.541±0.010	58.13±0.66	712±49	1.1±0.2	2.17±0.05	2.24
No anneal: TPC	5.40±0.07	0.550±0.008	48.16±0.39	339±15	1.12±0.22	1.43±0.03	1.46
TPC: Anneal	6.81±0.07	0.550±0.008	61.6±0.95	919±94	0.95±0.24	2.32±0.04	2.38

Table S7: Photovoltaic performance parameters (average of 16 devices) of P3HT:PC_{71}BM devices with and without TPC incorporation

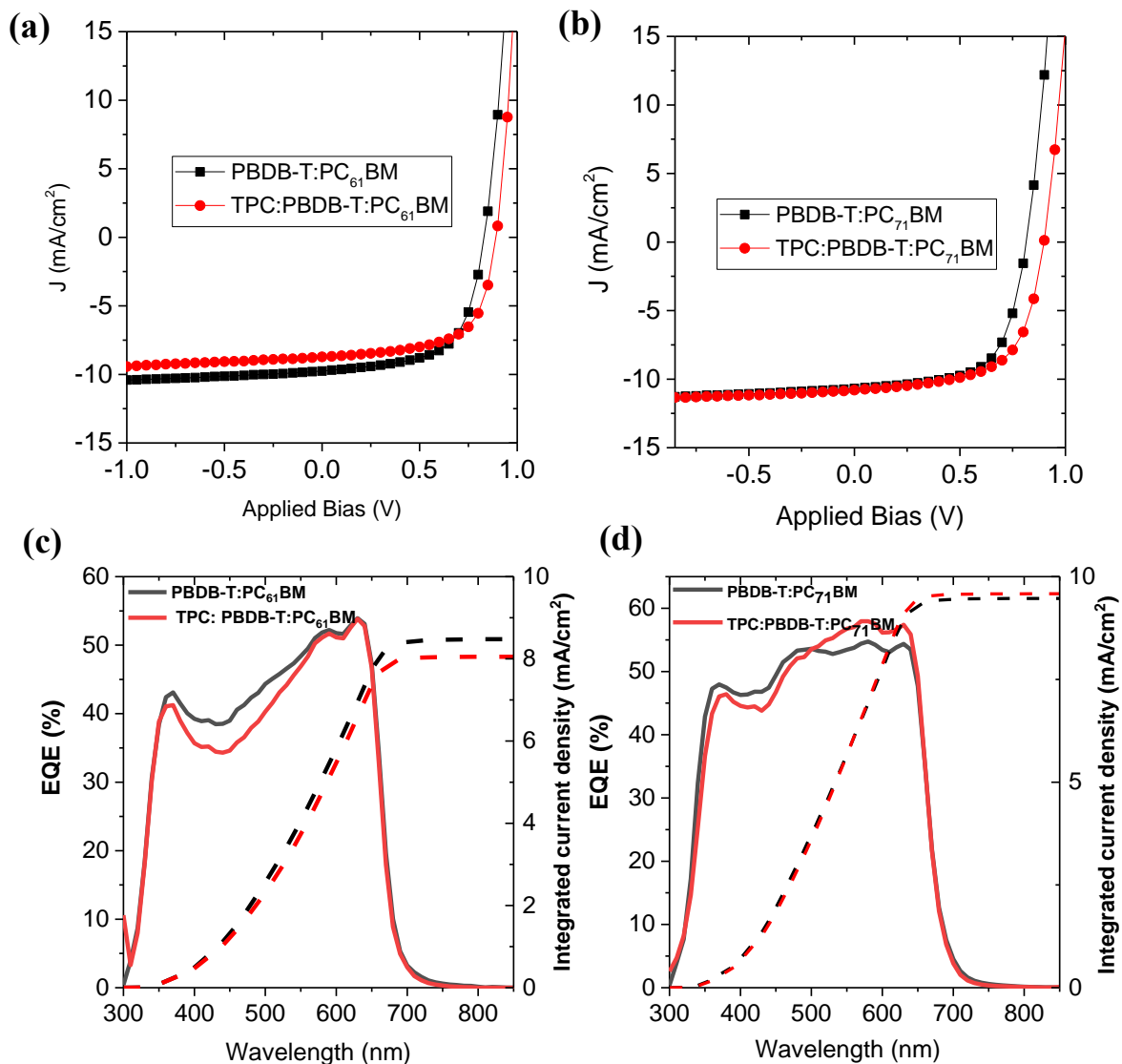| P3HT: PC_{71}BM	J_{sc} (mA/cm^2)	V_{oc} (V)	FF (%)	R_{sh} (Ωcm^2)	R_s (Ωcm^2)	PCE (%) avg.	PCE max (%)
No anneal	3.02±0.21	0.545±0.014	30.0±1.1	232±21	2.08±0.14	0.49±0.04	0.54
Anneal	8.05±0.33	0.547±0.005	53.04±0.89	627±89	0.98±0.22	2.33±0.08	2.45
No anneal: TPC	5.35±0.12	0.571±0.009	44.57±1.95	302±18	1.55±0.28	1.37±0.09	1.49
TPC: Anneal	8.06±0.14	0.554±0.004	59.02±0.76	958±157	0.99±0.24	2.64±0.04	2.74

Figure S13: J-V characteristics of the (a) PBDB-T: $PC_{61}BM$ and (b) PBDB-T:$PC_{71}BM$ solar cells with and without TPC incorporation. The corresponding EQE spectra and the integrated current density plots are shown in (c) and (d).

For PBDB-T:$PC_{61}BM$ blends with and without TPC additive, the integrated current density obtained from the EQE spectra are respectively 8.5 and 8.1 mA/cm^2. In the case of PBDB-T:$PC_{71}BM$ blends with and without TPC additive, the calculated integrated current density

values obtained from EQE spectra are 9.5 and 9.7 mA/cm^2 . In both cases the estimated current

density values from the EQE spectra are close to the measured J_{sc} values as shown in Table S8.

Table S8: Photovoltaic performance parameters (average of 16 devices) of PBDB-T:PCBM

devices with and without TPC incorporation

Blend	J_{sc} (mA/cm^2)	Voc (V)	FF(%)	R_{sh} (ohm.cm^2)	Rs (ohm cm^2)	PCE avg. (%)	PCE best (%)
PBDB-:PC$_{61}$BM	9.31±0.41	0.820±0.008	59.3±3.23	1080±190	3.10±1.66	4.53±0.39	5.06
PBDB-:PC$_{61}$BM With TPC	8.57±0.18	0.882±0.007	62.6±1.5	1223±401	2.25±0.57	4.73±0.18	4.95
PBDB-:PC$_{71}$BM	10.7±0.17	0.812±0.004	56.6±5.2	846±164	3.03±2.23	4.94±0.43	5.51
PBDB-:PC$_{71}$BM With TPC	10.8±0.05	0.900±0.006	60.4±2.18	947±318	3.15±1.23	5.87±0.18	6.04

P3HT and PBDB-T were selected as the donor molecule since it has a much higher LUMO of ~ -

3.0 eV and 2.92 eV compared to the fullerene molecules for which the LUMO is ~ -4 eV. For

both blends the optimum weight ratio of TPC was 7.5 mg/mL for the blend with PC$_{61}$BM

fullerene and 12.5 mg/mL for the blend with PC$_{71}$BM fullerene. Since P3HT:PCBM blend

requires a thermal annealing process to maximise the solar cell performance, which in turn may

obscure the TPC incorporation effects, solar cells were fabricated with and without thermal

annealing processing. Figure S12 (a) & (b), Table S6 and Table S7 shows the J-V characteristics and the photovoltaic performance parameters of the P3HT:$PC_{61}BM$ and P3HT:$PC_{71}BM$ blend films with and without TPC incorporation. TPC addition increases the PCE of both P3HT:$PC_{61}BM$ and P3HT:$PC_{71}BM$ blends irrespective of the thermal annealing process during device fabrication. However the improvement in solar cell performance is more pronounced when there is no annealing involved during the fabrication. The enhancement in V_{oc} upon TPC incorporation is ~ 60 and 30 meV for non-annealed blends of P3HT:$PC_{61}BM$ and P3HT:$PC_{71}BM$ respectively. In the case of a thermally annealed blend, instead of V_{oc}, a clear enhancement is observed for FF for both P3HT:$PC_{61}BM$ and P3HT:$PC_{71}BM$ blends. The thermal annealing induced orientation change (from edge on to face on) of P3HT molecules and its influence on increasing the V_{oc} has been previously well reported.[5] The observed increase in V_{oc} for the non-annealed blends of P3HT:$PC_{61}BM$ and P3HT:$PC_{71}BM$ due to TPC addition clearly agrees with the EA change of the fullerene molecules as shown by the CV measurements.

In the case of PBDB-T:PCBM blends, 20 % of PCE enhancement is observed for the PBDB-T:$PC_{71}BM$ when TPC is added and whereas no improvement in PCE is observed for PBDB-T:$PC_{61}BM$ blends when TPC is incorporated. This suggests that for different D-A blends separate optimization may be needed to maximise the solar cell device performance. However it is worth to note that, Voc increases by ~ 60 meV for PBDB-T:$PC_{61}BM$ and by ~ 80 meV for PBDB-T:$PC_{71}BM$ upon TPC incorporation thus confirming the LUMO level shift of fullerene molecules by TPC.
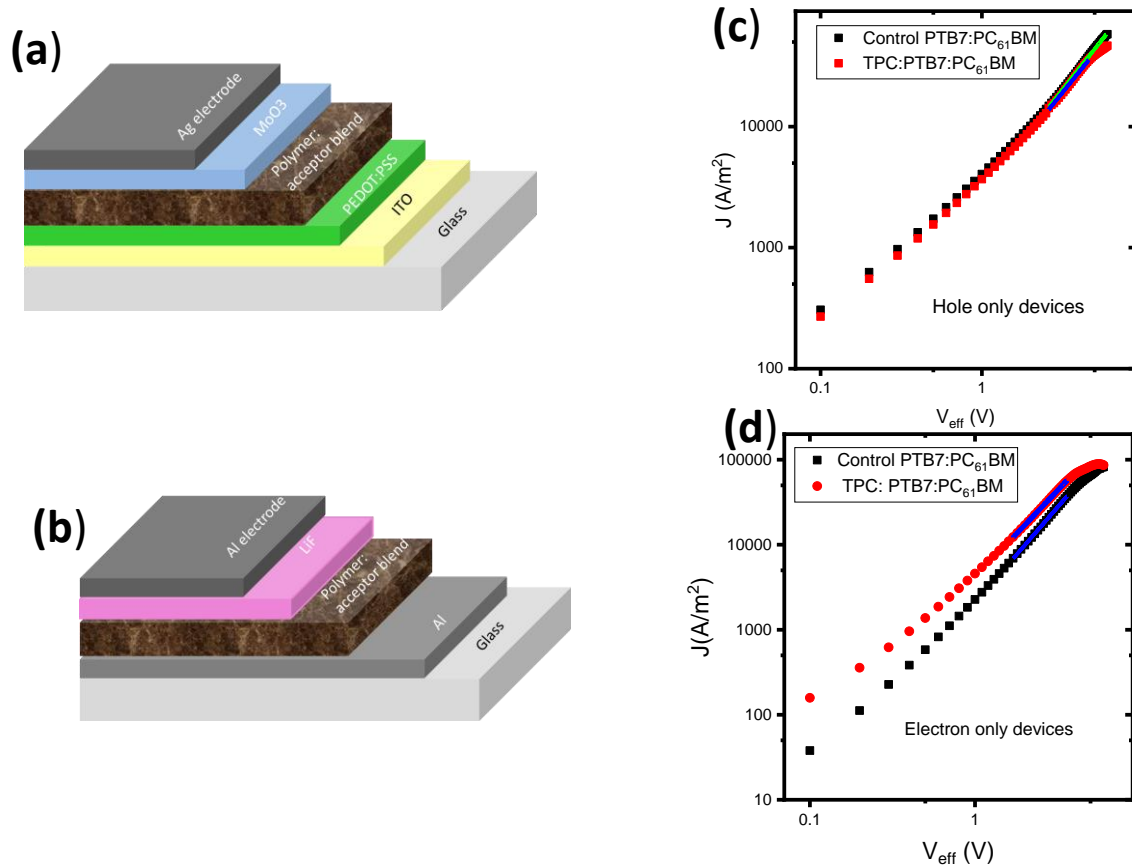
Figure S14: (a) Device structure used for measuring the hole mobility of PTB7:PC$_{61}$BM blends with and without TPC. (b) Device architecture used for measuring the electron mobility of PTB7:PC$_{61}$BM blends with and without TPC. (c) Fitted (blue and green lines) J-V characteristics of the hole only devices for PTB7:PC$_{61}$BM blends with and without TPC. (d) Fitted (blue lines) J-V characteristics of the electron only devices for PTB7:PC$_{61}$BM blends with and without TPC.

To study how the TPC incorporation is affecting the charge transporting properties of the PTB7:PCBM blend, the hole and electron mobility in the blend films were estimated using the

space charge limited current (SCLC) method. The structure of hole only devices are ITO/PEDOT:PSS/active layer blend/MoO$_3$/Ag and the structure of the electron only devices are Al/ active layer blend /LiF/Al as shown in Figure S14 (a) & (b)). The J-V curves of the hole only and electron only devices of PTB7:PCBM blends with and without TPC added are shown in Figure S14 (c) and (d). The mobility of holes and electrons are estimated using the Mott-Murgatroyd relation[6]:

$$J_{sclc} = \frac{9}{8}\varepsilon\mu\frac{V^2}{L^3}$$

where J_{sclc} is the steady state current density as a function of applied effective voltage V; L is the film thickness, ε is the dielectric constant of the organic semiconductors (set as 3.5), and μ represents the mobility.
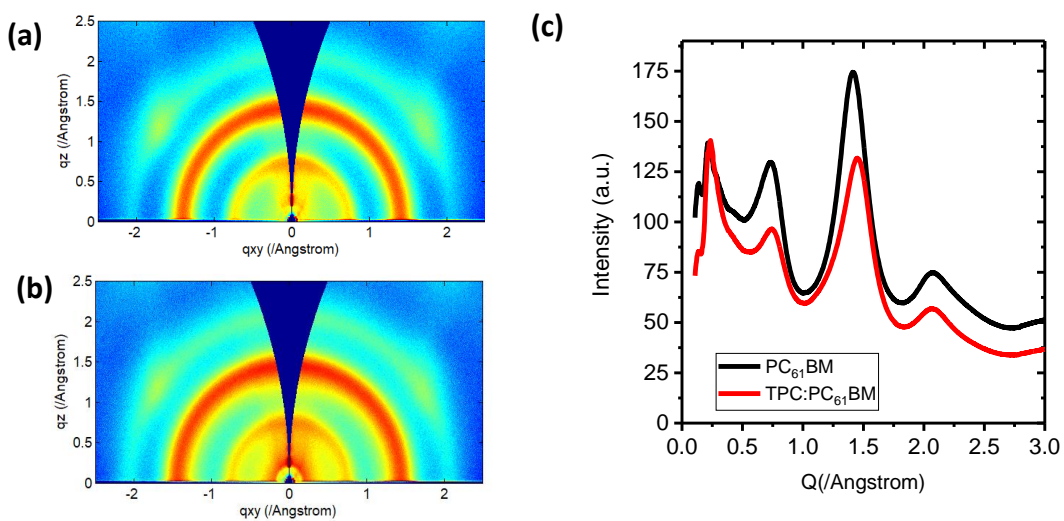
(a)

(b)

(c)

Figure S15: 2D-GIWAX data for the (a) neat $PC_{61}BM$ and (b) $PC_{61}BM$ films with TPC added; (c) the corresponding circularly integrated 1D GIWAX data.
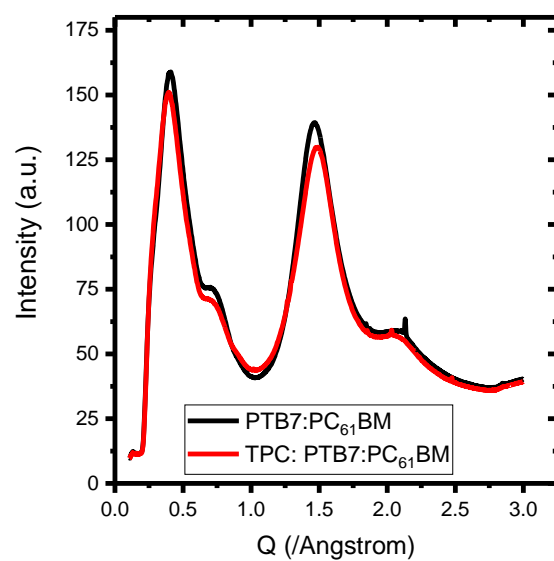
Figure S16: Circularly integrated one dimensional GIWAX data for the neat and TPC added PTB7:PC$_{61}$BM blends

Table S9. Parameters extracted from GIWAXS. Relative peak intensity and peak width is calculated from a quantitative peak fitting routine described in Experimental Details section. Peak positions are estimated from a visual inspection of the circularly integrated data. – indicates insufficient data due to peak overlap. The difference in PCBM 2nd peak position between neat

		PTB7 alkyl peak	PTB7 π-π stacking peak	PCBM 1st peak	PCBM 2nd peak
Relative peak intensity (from fits)	Blend as-cast	1.00	0.32	0.62	0.65
	Blend with TPC	0.93	0.42	0.65	0.63
FWHM (Å^{-1}) (from fits)	Blend as-cast	0.10	0.22	0.15	0.11
	Blend with TPC	0.11	0.36	0.17	0.12
Peak position (Å^{-1}) (from visual inspection)	Blend as-cast	0.41	–	–	1.47
	Blend with TPC	0.39	–	–	1.49
	PCBM as-cast	N/A	N/A	0.74	1.42
	PCBM with TPC	N/A	N/A	0.75	1.46

and blend films is likely an artefact due to overlap with the PTB7 π-π stacking peak but may also be related to the influence of PTB7 on PCBM structure.
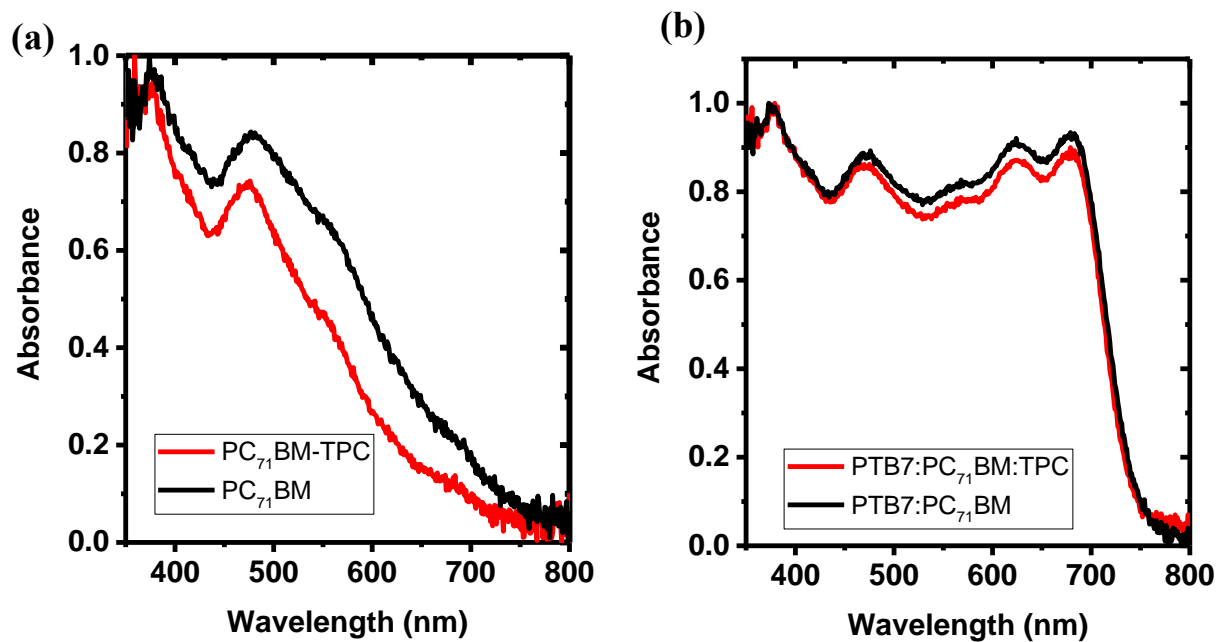
Figure S17. (a) The UV-VIS absorption spectra of $PC_{71}BM$ and (b) PTB7-$PC_{71}BM$ blend films with and without TPC.
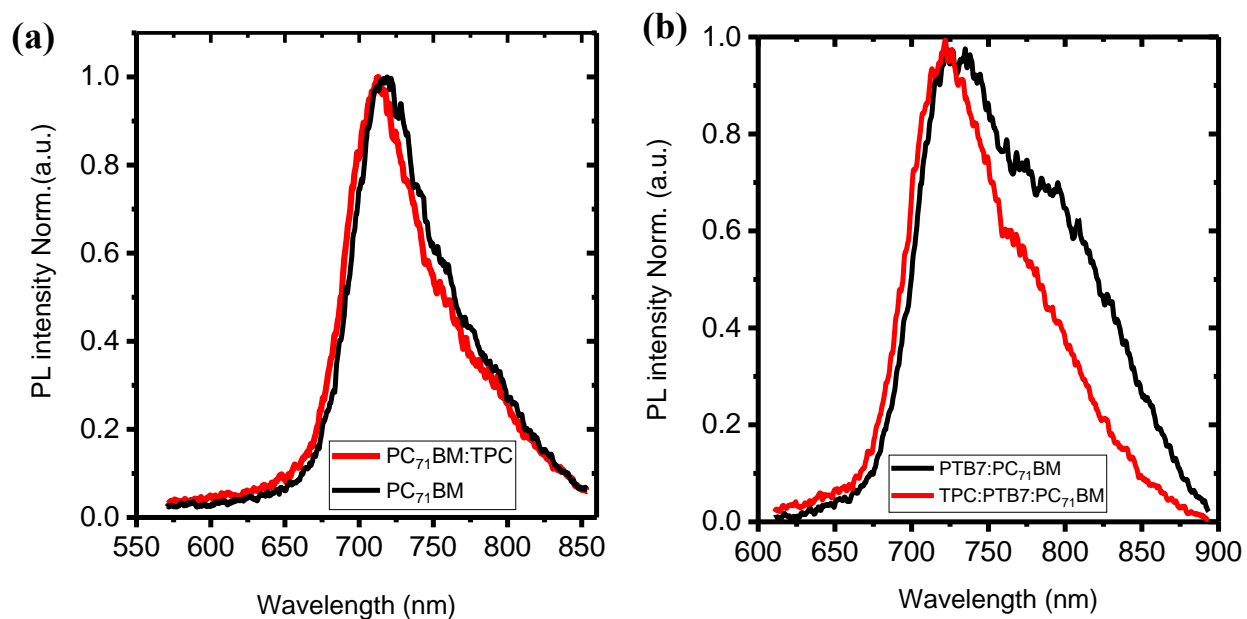
Figure S18: a) Steady state PL emission spectra of $PC_{71}BM$ thin films with and without added TPC (b) Steady state PL emission spectra of $PTB7:PC_{71}BM$ blend films with and without added TPC.
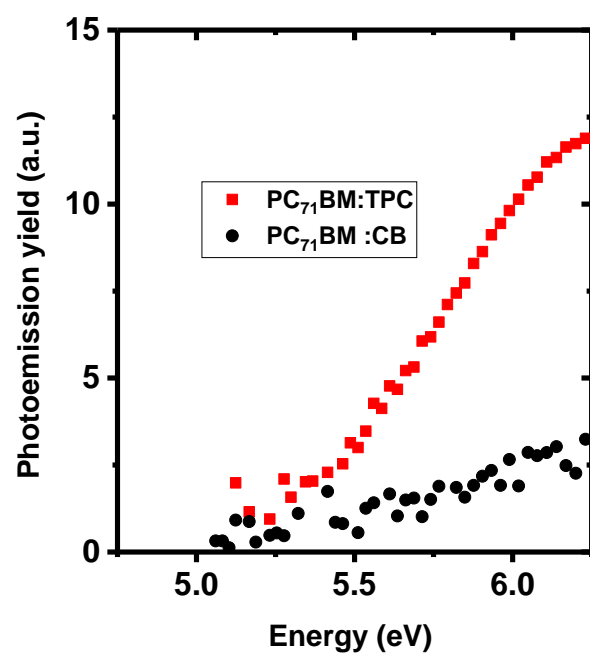
Figure S19: Air photoemission spectra of neat and TPC containing acceptor $PC_{71}BM$ thin films
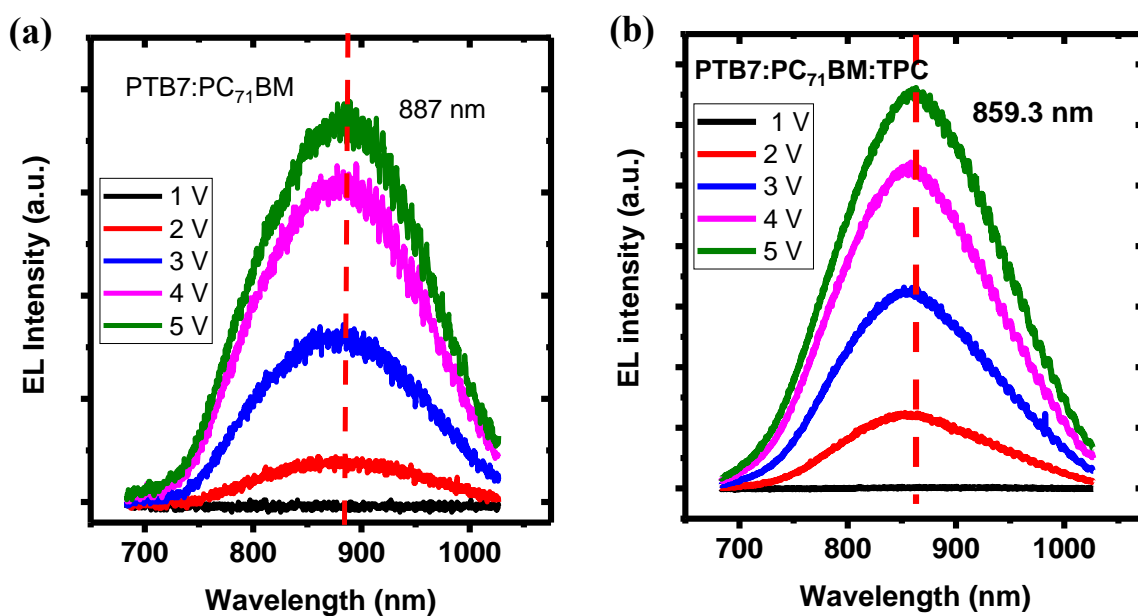
Figure S20. Electroluminescence spectra of the (a) PTB7-PC$_{71}$BM and (b) TPC:PTB7:PC$_{71}$BM
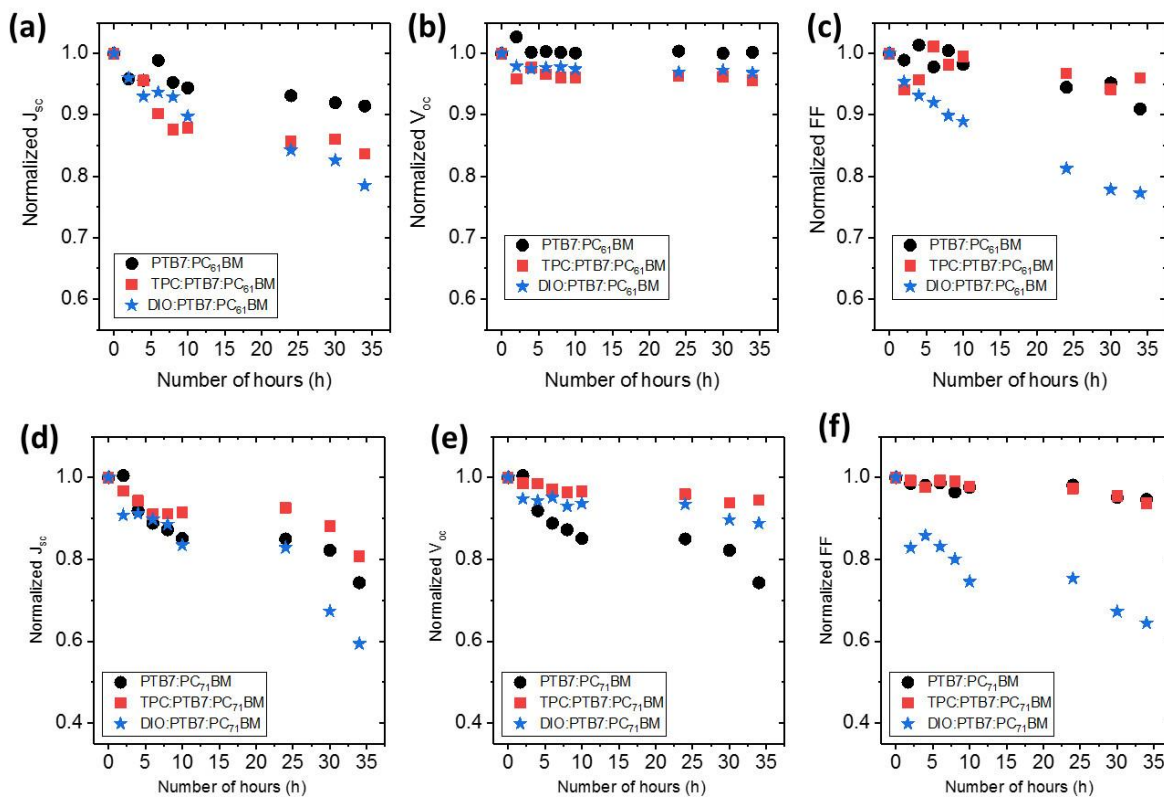
blend based OPV devices.

Figure S21: (a)-(c) Variation of photovoltaic performance parameters (J_{sc}, V_{oc} and FF) as a function of solar simulator exposure time for PTB7:$PC_{61}BM$ solar cells and (d) – (f) Variation of photovoltaic performance parameters (J_{sc}, V_{oc} and FF) as a function of solar simulator (1 Sun) exposure time for PTB7:$PC_{71}BM$ solar cells.
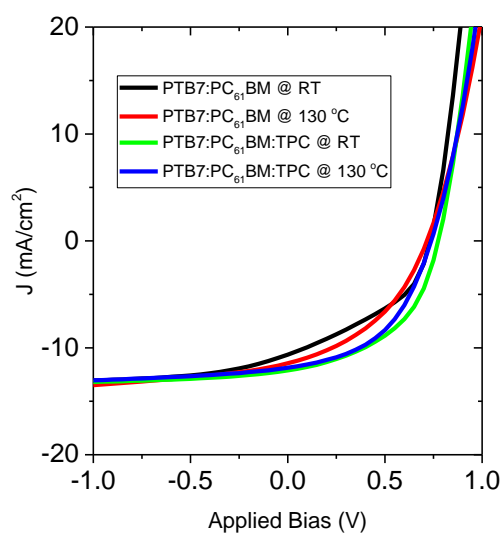
Figure S22: J-V characteristics of the solar cells showing the thermal annealing response of the PTB7:PC$_{61}$BM blend based solar cells with and without TPC added.

Table S10: Thermal stability comparison of the PTB7:PC$_{61}$BM blends with and without TPC added.

Blend	Annealing temperature (^{o}C)	J$_{sc}$ (mA/cm^2)	V$_{oc}$(V)	FF (%)	PCE Avg. (%)	PCE Best (%)
PTB7:PC$_{61}$BM	RT	10.2±0.4	0.725±0.025	39.1±1.40	2.88±0.26	3.16
PTB7:PC$_{61}$BM	130	10.5±0.5	0.719±0.007	41.3±1.0	3.13±0.12	3.35
PTB7:PC$_{61}$BM:TPC	RT	11.3±0.56	0.770±0.005	47.6±0.63	4.15±0.3	4.50
PTB7:PC$_{61}$BM:TPC	130	11.4±0.4	0.733±0.003	46.6±0.8	3.88±0.20	4.17

References

1. Cowan, S. R.; Roy, A.; Heeger, A. J., Recombination in Polymer-Fullerene Bulk Heterojunction Solar Cells. *Phys. Rev. B* **2010,** *82*, 245207.
2. Koster, L. J. A.; Mihailetchi, V. D.; Ramaker, R.; Blom, P. W. M., Light Intensity Dependence of Open-circuit Voltage of Polymer : Fullerene Solar Cells. *Appl. Phys. Lett.* **2005,** *86*, 123509.
3. Sworakowski, J., How Accurate are Energies of HOMO and LUMO Levels in Small-Molecule Organic Semiconductors Determined from Cyclic Voltammetry or Optical spectroscopy? *Synth. Met.* **2018,** *235*, 125-130.
4. Sworakowski, J.; Lipiński, J.; Janus, K., On the Reliability of Determination of Energies of HOMO and LUMO Levels in Organic Semiconductors from Electrochemical Measurements. A simple Picture Based on the Electrostatic Model. *Org. Electron.* **2016,** *33*, 300-310.
5. Verploegen, E.; Mondal, R.; Bettinger, C. J.; Sok, S.; Toney, M. F.; Bao, Z., Effects of Thermal Annealing Upon the Morphology of Polymer–Fullerene Blends. *Adv. Funct. Mater.* **2010,** *20*, 3519-3529.
6. Blakesley, J. C.; Castro, F. A.; Kylberg, W.; Dibb, G. F. A.; Arantes, C.; Valaski, R.; Cremona, M.; Kim, J. S.; Kim, J.-S., Towards Reliable Charge-Mobility Benchmark Measurements for Organic Semiconductors. *Org. Electron.* **2014,** *15*, 1263-1272.